EPJ manuscript No.
(will be inserted by the editor)

Photoexcitation of Baryon Resonances on Nucleons and Nuclei

An example: recent results from photoproduction of η mesons

B. Krusche[1], I. Jaegle[1], and T. Mertens[1] for the CBELSA/TAPS collaboration

Department of Physics and Astronomy, University of Basel, Ch-4056 Basel, Switzerland

Received: date / Revised version: date

Abstract. Photoproduction of η mesons off the proton, the deuteron and other light nuclei, and off heavy nuclei has been studied in detail during the last decade at the electron accelerators MAMI in Mainz, ELSA in Bonn, ERSF in Grenoble, CEBAF in Newport News, at KEK, and at Tohoku. The physics topics range from the detailed investigation of the properties of known nucleon resonances (in particular $S_{11}(1535)$), over the search of new states, to the in-medium properties of baryon resonances, and the possible formation of η - nucleus (quasi)bound states (η-mesic nuclei). It is thus an excellent example for the different aspects of the photoexcitation of nucleon resonances. Here we report new results from the CBELSA/TAPS experiment for this reaction at higher incident photon energies for the deuteron and heavy nuclei.

PACS. 13.60.Le meson production – 25.20.Lj photoproduction reactions

1 Introduction

The photoexcitation of baryon resonances is connected to two important aspects of non-perturbative, low-energy QCD. The excitation spectrum of the free nucleon itself is far from being understood. In particular, it is still not known if the problem of 'missing resonances' is caused by experimental bias or if baryon models use inapt effective degrees of freedom. This problem is sketched in Fig. 1 where the experimentally observed excitation spectrum [1] is compared to the predictions from typical quark model calculations [2]. Two problems are evident: the ordering of some of the lowest lying states is not reproduced. In particular, the lowest lying $N^\star$, the $P_{11}(1440)$ ('Roper') resonance and the lowest lying excited Δ, the $P_{33}(1600)$, which in the quark model belong to the N=2 oscillator shell, appear below the states from the N=1 shell. This is a severe problem for almost all quark models. Furthermore, many more states are predicted than have been observed, and the observed states are mostly clustered into a few narrow bands, a pattern which is not apparent for the quark model results. Most excited nucleon states have been first observed with hadron induced reactions, in particular elastic scattering of charged pions. It is thus possible that the data base is biased for states that couple only weakly to πN. However, the large progress in accelerator and detector technology made during the last two decades, now allows to study the electromagnetic excitation of resonances via photon induced reactions with comparable precision, although the cross sections are typically smaller by two orders of magnitude. These experiments have developed into two directions: measurements of photon induced

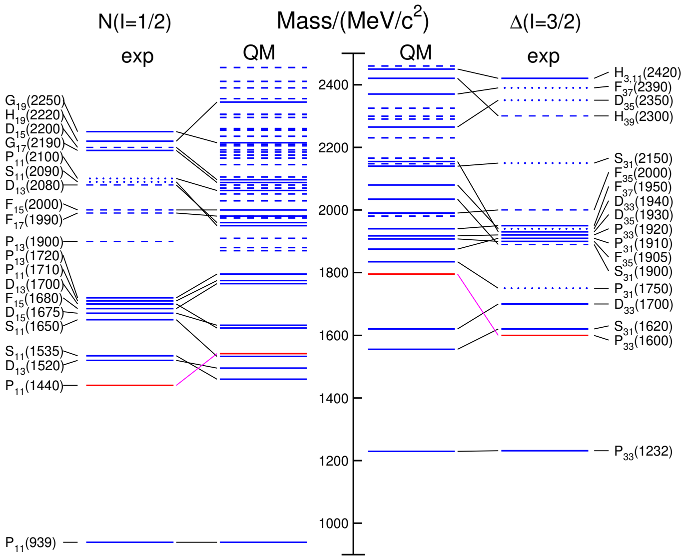

Fig. 1. Excitation scheme of the nucleon. Left hand side: isospin $I = 1/2$ N-states, right hand side: isospin $I = 3/2$ Δ-states. States labeled 'exp': experiment (Review of Part. Prop. [1]), full lines: three or four stars, dashed: two, dotted: one star. States labeled 'QM': quark model [2], all states N=1,2 bands, low lying states N=3,4,5. Full lines: (tentative) assignment to observed states, dashed lines: no observed counterparts.

meson production reactions up to high excitation energies and for many different nucleon - meson final states with the aim to identify at least some of the 'missing' states (see e.g. [3]) and precise investigations of the properties of known low lying nucleon resonances (see e.g. [4]).

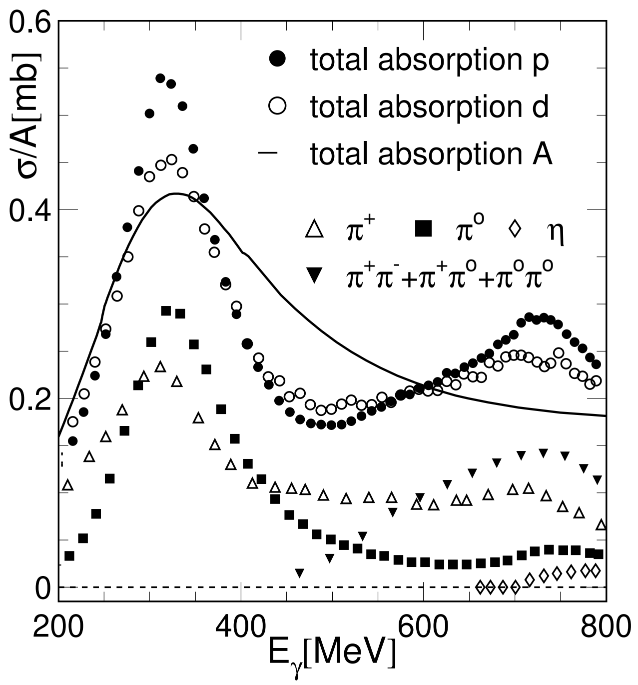

Fig. 2. Excitation functions for total photoabsorption off the proton [5], the deuteron [6] and the average for nuclei [7]. Also shown are the partial meson production cross sections for the proton [8–15] .

The other QCD aspect are the in-medium properties of hadrons, which are hotly discussed. Unlike any other composite systems, hadrons are objects, which are build out of constituents with masses (5 - 15 MeV for u,d quarks) that are negligible compared to the total mass. Most of the mass is generated by dynamical effects from the interaction of the quarks and an important role is played by the spontaneous breaking of chiral symmetry, the fundamental symmetry of QCD. The symmetry breaking, which is connected to a non-zero expectation value of scalar $q\bar{q}$ pairs in the vacuum, the chiral condensate, is reflected in the hadron spectrum. Without it, hadrons would appear as mass degenerate parity doublets, which is neither true for baryons nor for mesons. However, model calculations (see e.g. Ref. [16]) indicate a temperature and density dependence of the condensate, which is connected to a partial restoration of chiral symmetry. Although there is no direct relation between the quark condensate and the in-medium properties of hadrons (masses, widths etc.), there is an indirect one via QCD sum rules, which connect the QCD picture with the hadron picture. In the latter, the in-medium modifications arise from the coupling of mesons to resonance - hole states and the coupling of the modified mesons to resonances. Recently, Post, Leupold, and Mosel [17] have calculated the hadron in-medium spectral functions for π-, η-, and ρ-mesons and baryon resonances in a self-consistent coupled channel approach.

Experimentally, one of the clearest, although still not fully explained, in-medium effects has been observed in the excitation function of the total photoabsorption reaction (TPA). This is shown in Fig. 2, where the TPA off the proton [5] and the deuteron [6] are compared to the average of the nuclear cross sections [7], all normalized to the mass numbers A. The bump in the elementary cross sections around 700 MeV incident photon energy, which corresponds to the excitation of the $P_{11}(1440)$, $D_{13}(1520)$, and $S_{11}(1535)$ resonances, is not seen in the nuclear data. Many different effects have been discussed in the literature. They include trivial ones like nuclear Fermi motion, which certainly contributes to the broadening of the structure, but cannot explain its complete disappearance. Collisional broadening of the resonances due to additional decay channels like $NN^{\star} \rightarrow NN$ has been studied in detail in the framework of transport models of the Boltzmann-Uehling-Uhlenbeck (BUU) type (see e.g. [18]), but can also not fully explain the data. The situation is complicated since already on the free nucleon the so-called second resonance bump consists of a superposition of reaction channels with different energy dependencies (see Fig. 2). Inclusive reactions like TPA alone do not allow to study in-medium properties of individual nucleon resonances. A study of the partial reactions channels is desirable, but their experimental identification is more involved, and final state interaction effects (FSI) [21] as well as experimental bias due to the averaging over the nuclear density [20] must be accounted for (see Ref. [19] for a recent summary). Of special interest are meson production reactions which are dominated in the energy region of interest by one of the three resonances. Single and double pion production reactions have been employed for the study of the D_{13} resonance in the nuclear medium [22,23], although up to now without conclusive results.

In this paper we will discuss new results for the photoproduction of η-mesons, which can address interesting aspects of both, the study off excited states of the free nucleon and the in-medium properties of nucleon resonances.

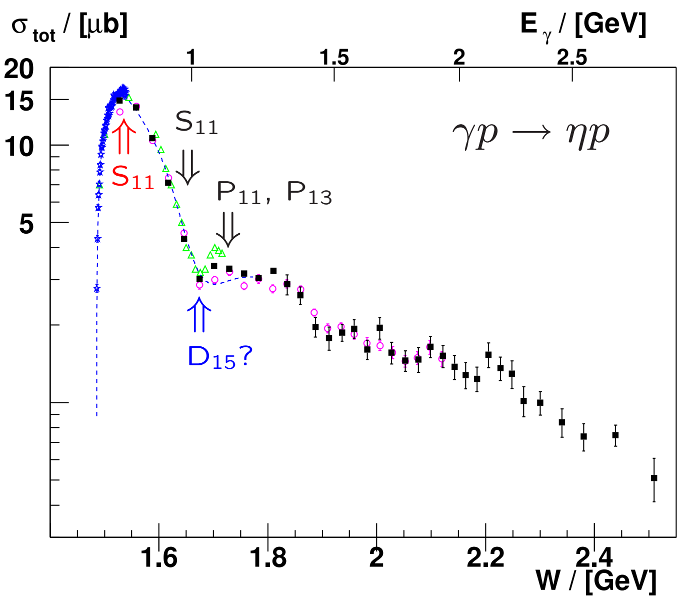

Fig. 3. Excitation function for photoproduction of η-mesons off the proton [10,24–26].

The excitation function of η photoproduction of the free proton is shown in Fig. 3. From threshold throughout the second resonance region it is completely dominated by the $S_{11}(1535)$ resonance [19,27] ($N\eta$ decay branching ratio $\approx 50\%$ [1]), there is some influence of an interference between the excitation of the $S_{11}(1535)$ and $S_{11}(1650)$ resonances and only a very weak contribution from the $D_{13}(1520)$ ($N\eta$ decay branching ratio $\approx 0.23\%$ [1]). An analysis of η photo- and electroproduction data in the framework of an isobar model [28] revealed weak contributions of four further resonances up to excitation energies of 1700 MeV and a recent combined analysis of η- and π-photoproduction reports contributions of another four states between W= 2000 - 2200 MeV [26].

2 Photoproduction of η-mesons off the neutron

The study of η photoproduction off the neutron aims at the investigation of the isospin structure of the electromagnetic excitation of resonances. Due to the non-availability of free neutron targets, photoproduction off light nuclei, in particular the deuteron, must be explored. The investigation of quasifree and coherent η photoproduction off ^{2}H and ^{3,4}He [29–35] has clarified the isospin structure of the $S_{11}(1535)$ electromagnetic excitation, which was found to be dominantly iso-vector (see [4] for a summary) and in addition provided interesting insights into the η - nucleus interaction. Typical results for the neutron/proton cross section ratio are summarized in Fig. 4. In the region of the $S_{11}(1535)$ it is almost constant around a value of 2/3. The slight rise to very low energies results from a breakdown of the participant - spectator picture at energies below the production threshold on the free nucleon. A quantitative analysis of all measurements results in a value of $|A^n_{1/2}|/|A^p_{1/2}| = 0.82 \pm 0.02$ for the ratio of the electomagnetic helicity couplings of the $S_{11}(1535)$ [34, 23].

At energies above the $S_{11}(1535)$ models predict a significant rise of the ratio due to the contribution of higher lying resonances (see Fig. 4 [28]). In the work of Chiang et al. [28] ('Eta-MAID'), the largest contributions comes from the $D_{15}(1675)$ resonance, which is known to have a stronger electromagnetic coupling to the neutron than to the proton [1]. However, the model uses a decay branching ratio of this resonance to $N\eta$ of 17 %, while the Particle Data Review quotes (0$\pm$1) % [1]. On the other hand, also in the framework of the chiral soliton model [36] a state is predicted in this energy range, with has much stronger photon couplings to the neutron than to the proton and a large decay branching ratio into $N\eta$. This state is the nucleon-like member of the predicted anti-decuplet of pentaquarks, which would be a P_{11} state. Therefore it would be very interesting to extend the data into the region of incident photon energies around 1 GeV.

In the following we will discuss preliminary results from a measurement of quasifree η photoproduction off neutrons and protons bound in the deuteron. The experiment was done at the Bonn ELSA accelerator with the combined Crystal Barrel [37] and TAPS [38,39] detectors. The η mesons were detected via the $\eta \rightarrow 3\pi^0 \rightarrow 6\gamma$ decay chain. First the invariant masses of the three pions and then the overall invariant mass of the η were used for the identification. The recoil protons and neutrons were iden-

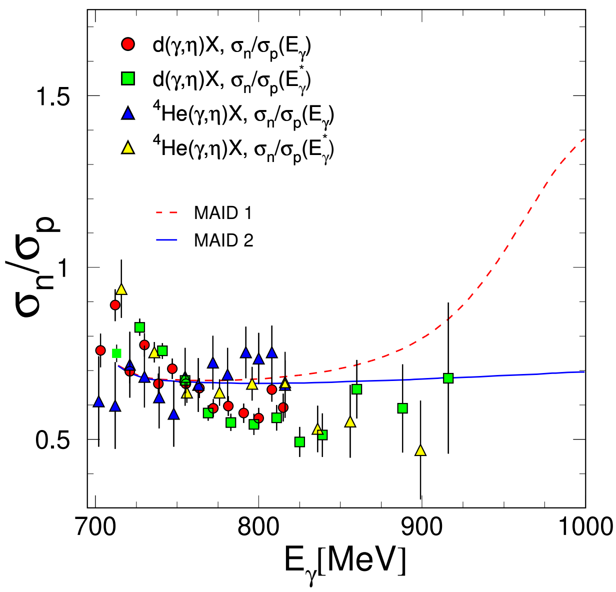

Fig. 4. Experimental results for the ratio for proton and neutron cross section measured with deuteron [34] and ^{4}He [31] targets compared to the prediction of Ref. [28] (curve labeled MAID 1) and from the same model if only $S_{11}(1535)$ contributes (curve labeled MAID2).

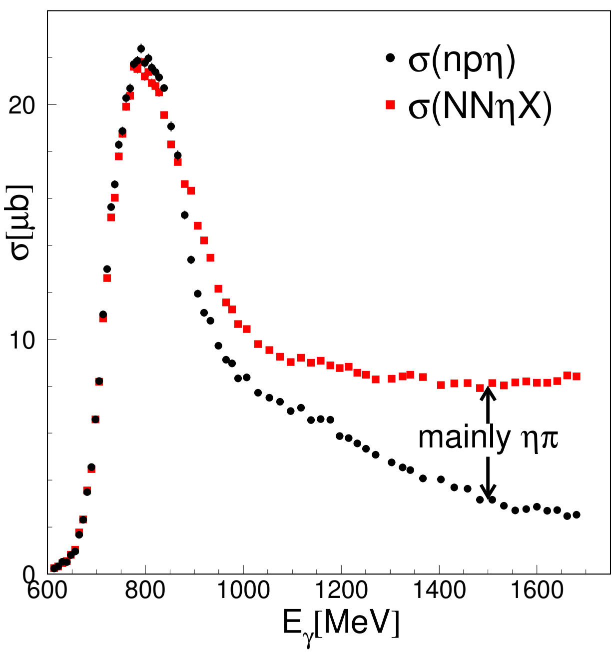

Fig. 5. Excitation functions for single η photoproduction ($\gamma d \rightarrow np\eta$) and the inclusive reaction $\gamma d \rightarrow NNX\eta$

tified with charged particle identification detectors and a time-of-flight versus energy analysis.

At incident photon energies above the $\eta\pi$ production threshold (930 MeV for the free nucleon, effectively lowered for the deuteron due to Fermi smearing) significant background from this channel appears. Part of it can be suppressed with the almost 4π solid angle coverage of the detector by the condition that not more than six photons and one recoil nucleon have been detected. However, there is still residual background for example from the final state $NN\eta\pi^{\pm}$ where the charged pion goes down the beam pipe or is misidentified as a proton, while a recoil neutron has escaped detection. This background was removed with a missing mass analysis based on the four-vectors of the six photons. For quasifree reactions off the deuteron, the missing mass peaks are only moderately broadened by Fermi smearing compared to the free nucleon case [13]. A comparison of the inclusive cross sections for the final states $np\eta$ and $NN\eta X$ is shown in Fig. 5.

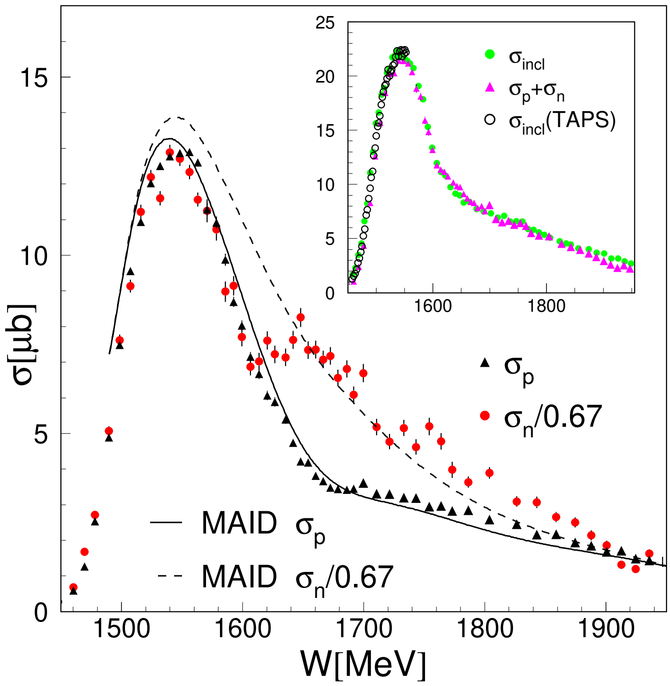

Fig. 6. Total cross sections for the final states ηp (σ_p, participant proton) and ηn (σ_n, participant neutron) normalized by 3/2 compared to the results of the MAID-model [28] folded with the momentum distribution of the bound nucleons. Insert: total inclusive cross section for the final state ηnp. Open symbols: results from Ref. [34], dots: present result, triangles: sum of quasifree exclusive cross sections $\sigma_p + \sigma_n$.

The results for the excitation functions of η photoproduction off the deuteron are summarized in Fig. 6. The cross section σ_{incl} corresponds to single quasifree η photoproduction off the deuteron, i.e. all events with an η identified by missing mass and production of further mesons excluded by missing mass were accepted. For the exclusive cross sections σ_p and σ_n coincident detection of a participant recoil proton, respectively recoil neutron, was required. The absolute normalization of the cross sections was obtained from the target thickness, the incident photon flux, the decay branching ratios ($\eta \rightarrow 3\pi^0$, $\pi^0 \rightarrow \gamma\gamma$), the detection efficiency of the η mesons and for the exclusive cross sections also the detection efficiencies of the recoil nucleons. The insert of Fig. 6 shows that the inclusive cross section agrees with previous results [29,34] available for incident photon energies below 800 MeV. Furthermore, the sum of the two exclusive cross sections agrees well with the total inclusive cross section, which is an additional test for the correctness of the efficiency correction applied for the recoil nucleon detection. The excitation functions for quasifree production off the proton and off the neutron shown in the main frame of the figure are in reasonable agreement with the predictions of the Eta-Maid model [28] folded with the nuclear momentum distribution. The excitation function off the neutron shows indeed a resonance structure around invariant masses of $W \approx 1675$ MeV, which is not seen for the proton. This is particularly clear in the ratio of the two cross sections shown in Fig. 7. It is close to 2/3 in the $S_{11}(1535)$ range, but then it peaks at an invariant mass around 1675, indicating the contribution of a resonance which couples much stronger to the neutron than to the proton. A similar structure has been reported from the GRAAL experiment [40] The analysis of the angular distributions, which may carry information about the quantum numbers of this resonance, is still under way.

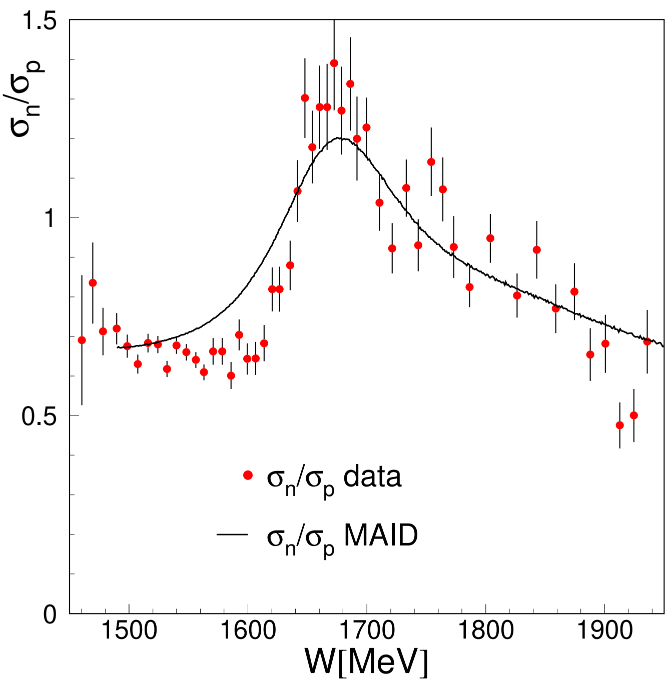

Fig. 7. Ratio of quasifree neutron and proton cross sections compared to the prediction of the Eta-MAID model [28] (folded with momentum distribution) as function of invariant mass W.

3 Photoproduction of η-mesons off nuclei

Photoproduction of η mesons in the second resonance region is an excellent tool for the study of the $S_{11}(1535)$ resonance, which completely dominates this reaction [10, 27]. A first search for possible in-medium effects on the S_{11} spectral function was done with the TAPS experiment at MAMI [41]. However, the experiment covered only incident photon energies up to 800 MeV, i.e. approximately up to the peak position of the resonance. The experimental results were in good agreement with BUU-model calculations (see e.g. [18]). Furthermore, an almost perfect scaling of the cross sections with $A^{2/3}$ ($A=$ nuclear mass number) was found, which indicates strong final state interaction effects. Subsequently, measurements at KEK [42] and Tohoku [43] extended the energy range up to 1.1 GeV. The KEK experiment reported some collisional broadening of the S_{11} resonance, however possible background from $\eta\pi$ final states, which can fake such a result, was neglected. The Tohoku experiment pointed to a significant contribution of a higher lying resonance to the $\gamma n \rightarrow n\eta$ reaction. However, none of these experiments covered the full line shape of the S_{11}.

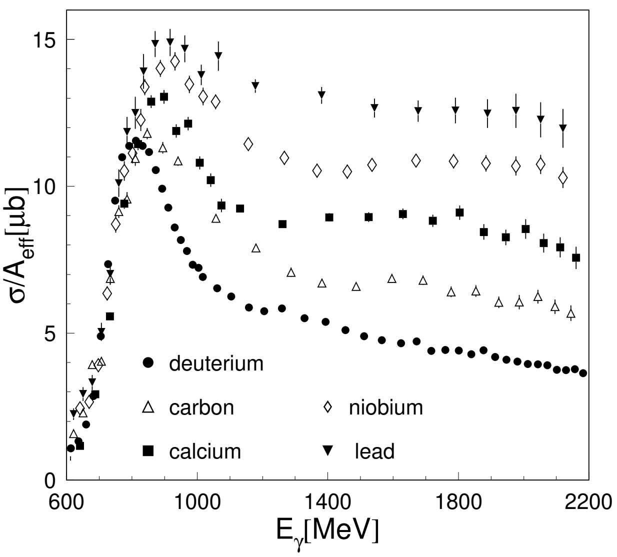

Fig. 8. Total inclusive (final state ηX, where X can also include pions) η photoproduction off the deutron and off nuclei from the present experiment, scaled by $A_{eff}=2$ for the deuteron and $A_{eff}=A^{2/3}$ for all other nuclei.

Preliminary results for η photoproduction off ^{2}H and off heavier nuclei from the Crystal Barrel/TAPS experiment at the Bonn ELSA accelerator are summarized in Fig. 8. The data agree with the previous results [41] at incident photon energies below 800 MeV, where they scale with $A^{2/3}$ (respectively A for the deuteron). This scaling changes at higher incident photon energies, where the cross sections are approximately proportional to A. It is clear from the discussion in sec. 2 that at this energies $\eta\pi$ final states contribute. However, there is no good reason why this contributions, which are also subject to strong FSI, should modify the scaling. Indeed, for the low energy regime it was shown in [23] that due to FSI all investigated reactions (η, single π, double π) obey approximately an $A^{2/3}$ scaling law. Another possibility would be that the η mean free path increases as function of η momentum, so that FSI for η mesons gets effectively weaker for higher incident photon energies. However, a detailed analysis of the scaling of the momentum-differential cross sections, which will be discussed elsewhere, points to another explanation. The η mean free paths seems to be fairly constant over a wide range of η momentum. However, at higher incident photon energies secondary processes e.g. of the type $\gamma N \rightarrow N\pi$, $\pi N \rightarrow \eta N$ become more and more important and these contribution increase of course as function of the mass number.

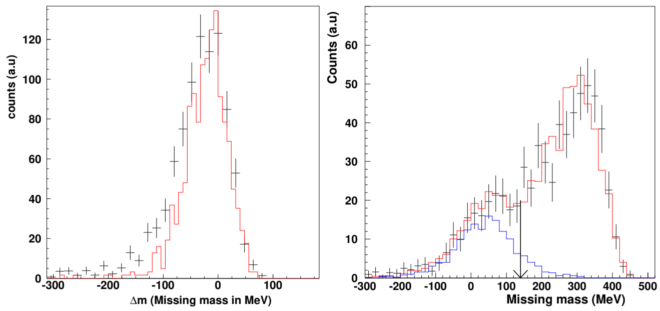

Fig. 9. Missing mass spectra for the measurement off lead nuclei for incident photon energies around 800 MeV (left hand side) and 1500 MeV (right hand side). The histograms are results of a BUU calculation [44] folded with the detector resolution.

Both effects, the contribution of $\eta\pi$ final states and the secondary η production processes, obscure the line shape of the S_{11} at photon energies above 800 MeV. A suppression of these contributions is again possible via cuts on the reaction kinematic, which are however much less selective than for the deuteron due to the stronger Fermi smearing. Typical missing mass spectra calculated under the assumption of quasifree single η photoproduction are shown in Fig. 9. The missing mass ΔM is given by:

$$\Delta M = \sqrt{(E_b + m_N - \sum_{i=1}^{6} E_{\gamma_i})^2 - (\boldsymbol{P_b} - \sum_{i=1}^{6} \boldsymbol{P_{\gamma_i}})^2} - m_N . \quad (1)$$

where E_{γ_i} and $\boldsymbol{P_{\gamma_i}}$ are energies and momenta of the decay photons and m_N is the nucleon mass. At low incident photon energies a clear peak centered around zero is visible, at higher energies a large contribution from $\eta\pi$ and secondary processes appears at positive missing energies. The distributions are in good agreement with results from the BUU model [44]. The indicated cut removes most of the unwanted contributions. Excitation functions for single, quasifree η photoproduction after the missing mass cut are shown in Figs. 10,11 for carbon and lead. They are compared to the average nuclear cross section, obtained from the deuteron data, folded with the momentum dis-

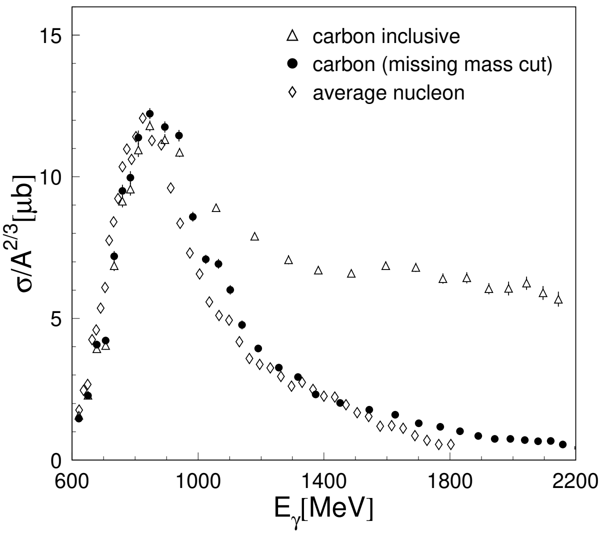

Fig. 10. Total cross section for η production off carbon. Inclusive excitation function for final states with at least one η and after a cut on reaction kinematics for single, quasifree η production compared to the Fermi smeared average neutron cross section.

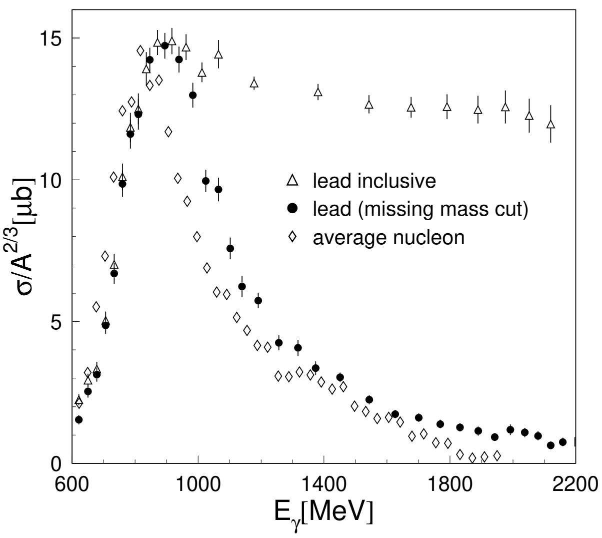

Fig. 11. Same as Fig. 10 for lead nuclei.

tributions of the nucleons bound in the heavy nuclei. Already these preliminary results show, that the in-medium spectral function of the S_{11} resonance is not strongly modified. In case of carbon, the data agree almost perfectly with the Fermi-smeared average nucleon data. There is no need for a significant collisional broadening, which was reported in [42] on the basis of data without kinematical cuts. The agreement for the lead data is less good, it would be consistent with some upward shift of the resonance position together with a broadening. However, in particular for lead the suppression of $\eta\pi$ final states and secondary processes by the missing mass cut is not perfect. A more detailed analysis of the data including a comparison to BUU predictions is still under way.

4 Acknowledgments

The experimental results have been obtained by the CB-ELSA/TAPS collaboration and are part of the PhD theses of I. Jaegle and T. Mertens. We gratefully acknowledge many stimulating discussions with U. Mosel and P. Mühlich (BUU results), and with L. Tiator (Eta-MAID). This work was supported by Schweizerischer Nationalfonds and Deutsche Forschungsgemeinschaft.

References

1. W.-M. Yao et al., J. Phys. **G33**, (2006) 1.
2. S. Capstick and W. Roberts, Phys. Rev. **D49** (1994) 4570; ibid. **D57**, (1998) 4301; ibid. **D58**, (1998) 074011.
3. V.D. Burkert and T.-S. Lee, Int. J. Mod. Phys. **E13** (2004) 1035.
4. B. Krusche and S. Schadmand, Prog. Part. Nucl. Phys. **51** (2003) 399.
5. T.A. Armstrong et al., Phys. Rev. **D5** (1972) 1640.
6. T.A. Armstrong et al., Nucl. Phys. **B41** (1972) 445.
7. N. Bianchi et al., Phys. Lett. **B325** (1994) 333.
8. K. Büchler et al., Nucl. Phys. **A570** (1994) 580.
9. A. Braghieri et al., Phys. Lett. **B363** 1995 46.
10. B. Krusche et al., Phys. Rev. Lett. **74** (1995) 3736.
11. M. MacCormick et al., Phys. Rev. **C53** (1996) 41.
12. F. Härter et al., Phys. Lett. **B401** (1997) 229.
13. B. Krusche et al., Eur. Phys. J. **A6** (1999) 309.
14. M. Wolf et al., Eur. Phys. J. **A9** (2000) 5.
15. W. Langgärtner et al., Phys. Rev. Lett. **87** (2001) 052001.
16. M. Lutz, S. Klimt, and W. Weise, Nucl. Phys. **A542**, (1992) 521.
17. M. Post, S. Leupold, and U. Mosel, Nucl. Phys. **A741**, (2004) 81.
18. J. Lehr, M. Effenberger, U. Mosel, Nucl. Phys. **A671**, (2000) 503.
19. B. Krusche, Prog. Part. Nucl. Phys. **55** (2005) 46.
20. J. Lehr and U. Mosel, Phys. Rev. **C64** (2001) 042202.
21. B. Krusche et al., Eur. Phys. J. **A22** (2004) 347.
22. B. Krusche et al., Phys. Rev. Lett. **86** (2001) 4764.
23. B. Krusche et al., Eur. Phys. J. **A22** (2004) 277.
24. F. Renard et al., Phys. Lett. **B528** (2002) 215.
25. M. Dugger et al., Phys. Rev. Lett. **89** (2002) 222002.
26. V. Crede et al., Phys. Rev. Lett. **94** (2005) 012004.
27. B. Krusche et al., Phys. Lett. **B397** (1997) 171.
28. W.-T. Chiang et al., Nucl. Phys. **A700** (2002) 429.
29. B. Krusche at al., Phys. Lett. **B358** (1995) 40.
30. P. Hoffmann-Rothe et al., Phys. Rev. Lett. **78** (1997) 4697.
31. V. Hejny et al., Eur. Phys. J. **A6** (1999) 83.
32. J. Weiss et al., Eur. Phys. J. **A11** (2001) 371.
33. V. Hejny et al., Eur. Phys. J. **A13** (2002) 493.
34. J. Weiss et al., Eur. Phys. J. **A16** (2003) 275.
35. M. Pfeiffer et al., Phys. Rev. Lett. **92** (2004) 252001.
36. R.A. Arndt et al., Phys Rev **C69** (2004) 035208.
37. E. Aker et al., Nucl. Instr. and Meth. **A321**, (1992) 69.
38. R. Novotny, IEEE Trans. on Nucl. Science **38**, (1991) 379.
39. A.R. Gabler et al., Nucl. Instr. and Meth. **A346**, (1994) 168.
40. V. Kuznetsov for the GRAAL collaboration, hep-ex/0409032 (2004).
41. M. Röbig-Landau et al., Phys. Lett. **B373** (1996) 45.
42. T. Yorita et al., *Phys. Lett.* **B476** (2000) 226.
43. T. Kinoshita et al., *Phys. Lett.* **B639** (2006) 429.
44. P. Mühlich, University of Giessen, private communication (2006).